SERBIAN JOURNAL OF ELECTRICAL ENGINEERING
Vol. 18, No. 2, June 2021, 255-270

UDC: 621.383.51: 621.317.32; 621.374 **DOI: https://doi.org/10.2298/SJEE2102255P**

C-V and I-V Characterisation of CdS/CdTe Thin Film Solar Cell Using Defect Density Model

Debashish Pal[1], Soumee Das[2]

Abstract: This paper presents a detailed study of the current-voltage (I-V) and capacitance-voltage (C-V) measurements made on a CdS/CdTe based solar cell by numerical modeling. Implementation of the simulated cell having a superstrate configuration was done with the help of SCAPS program using defect density model. The I-V characterisation includes window and absorber layer optimisation based on various factors including the impurity doping concentration, thickness and defect density. The energy band diagram, spectral response and current-voltage plot of the optimised cell configuration are shown. C-V characterisation (Mott-Schottky analysis) of the solar cell is conducted at different low frequencies to determine the flatband potential, carrier concentration and to validate the reliability of the results. The optimum device performance was obtained when the active layer was 2 μm thick with a doping level of $1\times10^{15}/cm^3$.

Keywords: CdS/CdTe, Conduction band offset, Debye length, Mott-Schottky plot, Numerical modeling, SCAPS-1D, Spectral response.

1 Introduction

CdTe is a group II-VI semiconductor material having excellent photovoltaic characteristics owing to its high absorption coefficient (greater than $5\times10^5/cm$) and direct optical bandgap (~1.5 eV) which is very close to the optimal bandgap of single junction solar cells [1 − 3]. Because the bandgap matches closely with the solar spectrum, therefore the thickness of active CdTe layer required for generating power is relatively lower compared to other semiconductors. Therefore, CdTe based solar cells offer an economical alternative to the present thin film technologies by employing low temperature deposition, reduced material usage, ease in device processing, lower production cost, time and energy [4 − 6]. In addition, CdTe solar cells have demonstrated long term stability and high efficiency under AM1.5G illumination condition [7 – 9].

One of the factors that severely impair the performance of CdTe solar cells is an inappropriate back contact. The formation of a stable back contact having low resistance and non-rectifying properties is thus imperative to overcome the

[1]Department of Material Science and Engineering, Tripura University, India; E-mail: pal.debashish@gmail.com
[2]IBM India Pvt. Ltd. Kolkata, India; E-mail: soumee.das@gmail.com

degradation in performance associated with solar cells [10 − 14]. CdTe is a semiconductor having a high electron affinity ($\chi = 4.5$ eV) and bandgap (~1.5eV). Therefore, the work function of the back contact must be greater than or equal to 6 eV to make a good ohmic contact. Unfortunately, most of the metals do not have such a high value of work function and form Schottky barrier contacts with CdTe. Even if a suitable metal is found having a reasonably high value of work function, the presence of surface states at the metal/CdTe interface may not form a good ohmic contact. The presence of a blocking barrier contact can have a significant effect on the current-voltage characteristics of the solar cell by hindering the flow of holes (rollover effect). An efficient way to overcome this design problem is to introduce a heavily doped electron back reflection (EBR) layer in between the CdTe absorber and metal back contact [11, 15]. Various candidates have been proposed as EBR in the past including, Zinc Telluride (ZnTe), Antimony Telluride (Sb_2Te_3), and Arsenic Telluride (As_2Te_3) [16 – 17].

The maximum theoretical efficiency for CdTe based solar cell at standard solar spectrum is about 29%. Recently a proposed structure of $SnO_2/Zn_2SnO_4/CdS/CdTe/As_2Te_3/Cu$ showed a conversion efficiency of 18.6% (V_{OC} = 0.92 V, J_{SC} = 24.97 mA/cm^2, and FF = 0.81) using AMPS-1D simulator [18]. AFORS-HET was used to investigate TCO/CdS(n-type)/CdTe(p-type)/ CdTe(p+-type)/metal structure solar cell which produced an efficiency of 19.83% [19]. An efficiency of 22.79%, open-circuit voltage of 0.987 V, a short-circuit current density of 27.9 mA/cm^2 and a fill factor of 82.4%, was reported for CdS/CdTe solar cell with step doped absorber layer, ZnTe optimized back surface field layer having a long carrier lifetime [20]. Researchers showed that the proposed structure of ZnO/CdS/CdTe/ZnTe demonstrated the highest efficiency of 24.66% (V_{OC} = 946.51 mV, J_{SC} = 34.40 mA/cm^2 and FF = 75.72%) under global AM1.5G illumination spectra using a one-dimensional simulation software, ADEPT 2.1 [21].

Numerical modeling of thin film solar cells is an important strategy to test the validity of proposed structures and to predict the effect of physical and material changes on the cell performance. The objective of this paper is to use the various parameters present in literature to determine the performance of a CdS/CdTe thin film solar cell, with emphasis on power conversion efficiency (PCE). In particular dependence of conversion efficiency on window and absorber layer thickness and doping concentration will be shown. Moreover, the results of theoretical capacitance-voltage measurements will be presented for the very first time, using the SCAPS-1D program, for a CdS/CdTe photovoltaic cell to calculate the flatband voltage and carrier density. Finally, with the optimised CdS/CdTe solar cell presented in this paper, comparisons will be drawn to related work in the past.

2 Device Design and Numerical Modeling

SCAPS-1D is a computer program used for modeling crystalline semiconductor devices, with emphasis on photovoltaic devices and is used as a simulation tool to understand the operation of solar cells yielding reliable results [22]. Simulations were performed under standard AM1.5G one sun illumination at an operating temperature of 300 K.

Fig. 1 shows the basic configuration of the solar cell under investigation.

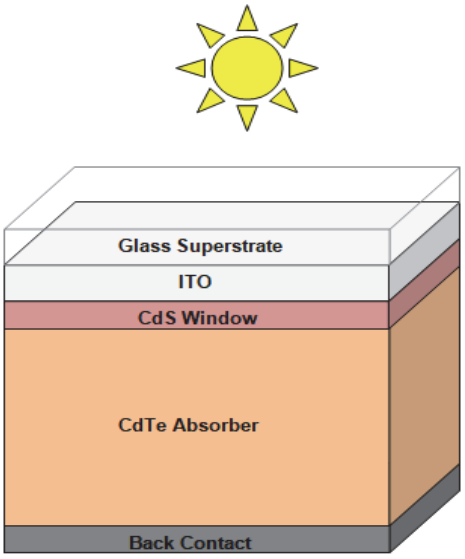

Fig. 1 – *Schematic diagram of the CdS/CdTe solar cell.*

The cell is composed of an ITO coated glass layer, where the ITO layer acts as a transparent conducting oxide. The TCO layer is the front contact of the solar cell. It should be highly transparent (more than 85% in the visible spectrum), should be very conductive at room temperature (low sheet resistance) and should have good adhesion to glass substrate. The ITO layer with a large bandgap of 3.6 eV is used to prevent optical losses and is sensitive to the ultra-violet (UV) light which constitutes about 3–5% of the total energy of the solar spectrum. The n-CdS film is an ideal candidate for the formation of a heterojunction, despite a lattice mismatch of 10% with p-CdTe layer, which aids in the separation of the photogenerated charge carriers. Together they form a type II heterojunction interface with the conduction band of one semiconductor lying above the conduction band level of the other semiconducting material. The heterojunction thus facilitates the transport of electrons from one conduction band to another improving the charge collection. The depletion region reaches deep into the CdTe material because the doping concentration of CdTe is lower compared to the TCO

and the n-CdS layer. The sunlight on reaching the depletion region generates electron-hole pairs within it which are separated due to the presence of built in electric field directed from CdS to CdTe layer. The initial factors highlighted in **Tables 1 and 2** for the numerical analysis were chosen after careful consideration [18 – 21], which shows the material and contact layer parameters respectively.

Table 1

Initial material parameters used in the simulation.

Parameters	ITO	n-type CdS	p-type CdTe
Thickness (μm)	0.1	0.05	0.5 – 3.0
Dielectric Constant	9.0	10.0	9.4
Energy Bandgap (eV)	3.6	2.4	1.5
Electron Afinity (eV)	4.5	4.5	4.3
Conduction Band DOS ($1/cm^3$)	2.2×10^{18}	2.2×10^{18}	8×10^{17}
Valence Band DOS ($1/cm^3$)	1.8×10^{19}	1.8×10^{19}	1.8×10^{19}
Electron Mobility (cm^2/Vs)	100	100	320
Hole Mobility (cm^2/Vs)	25	25	40
Donor Concentration ($1/cm^3$)	1×10^{18}	$5\times10^{18}/1\times10^{19}/5\times10^{19}$	–
Acceptor Concentration ($1/cm^3$)	–	–	5×10^{14} / 1×10^{15} / 5×10^{15}
Donor Defect Density ($1/cm^3$)	–	–	2×10^{11} to 2×10^{15}
Acceptor Defect Density ($1/cm^3$)	1×10^{15}	1×10^{15} to 1×10^{19}	–
Donor Defect Peak Energy (eV)	–	–	Midgap
Acceptor Defect Peak Energy (eV)	Midgap	Midgap	–
Electron Capture Cross-section ($1/cm^2$)	1×10^{-12}	1×10^{-17}	1×10^{-12}
Hole Capture Cross-section ($1/cm^2$)	1×10^{-15}	1×10^{-12}	1×10^{-15}

Table 2
Initial contact layer parameters used in the simulation.

Parameters	Front Contact	Back Contact
Barrier potential (eV)	Flatband	0.4
Electron Surface Recombination (cm/s)	1×10^{7}	1×10^{7}
Hole Surface Recombination (cm/s)	1×10^{7}	1×10^{7}

The base value of CdTe thickness was chosen as 1 μm while the impurity concentration and defect density of states of CdS and CdTe were set to 5×10^{18}, 5×10^{14} /cm^3 and 1×10^{15}, 2×10^{11}/cm^3 respectively.

3 Results and Discussion

3.1 Effect of thickness and doping concentration

CdS can be formed by employing several common low-cost techniques such as radio frequency sputtering, closed space sublimation and chemical bath deposition. On the other hand, CdTe layer can be deposited using techniques like electro-deposition, screen printing and close space sublimation. However, because of the inherent drawbacks associated with these conventional methods, several modified strategies are being explored which include low temperature deposition, all electrodeposited method [23].

The CdS layer is the window of the solar cell having donor impurities and is moderately conducting to reduce electrical losses associated with the solar cell. It should have relatively high transparency and should not be very thick. A thick CdS layer can hinder the absorption of photons by the CdTe absorber material. At the same time in order to avoid the possibility of short circuiting the window layer should not be too thin. For the solar spectral response to remain unaltered the CdS layer should be highly responsive and photoconductive. The bandgap of CdS is rather low (~2.4 eV) because of which it cannot absorb short wavelengths below 500 nm. Therefore, in order to improve the blue response of the solar cell the CdS thickness is chosen to be less than 100nm. The reduced absorption loss in the blue region of the spectrum improves the short-circuit current density and the conversion efficiency. Also, it is worth mentioning that considerable difficulty is encountered while fabricating CdS layers having thickness less than 50 nm. This is because thinner CdS layers can lead to the short circuit of TCO and the CdTe layer caused by the partial grain covering and pinholes in CdS which has an adverse effect on the open-circuit voltage and fill factor. Therefore, for the purpose of investigation the thickness of CdS layer is chosen to be 50 nm in accordance with practical values.

Table 3 shows the variation of the electrical parameters with the doping concentration in CdS layer at a fixed thickness of 50 nm. It is evident that there is no significant variation in any of the parameters with the change in the doping concentration. Therefore, for further analysis the doping concentration is chosen as $1x10^{19}$ atoms/cm^3.

Table 3

Effect of impurity doping concentration of CdS on the electrical parameters.

CdS Doping Conc. (1/cm^3)	V_{OC} (V)	J_{SC} (mA/cm^2)	FF (%)	Efficiency (%)
5×10^{18}	0.8969	25.395009	80.01	18.22
1×10^{19}	0.8967	25.405958	81.29	18.29
5×10^{19}	0.8965	25.426972	80.73	18.40

CdTe is the absorber layer of the solar cell which has acceptor doping ion concentration. It has an ideal bandgap (~1.5 eV) and high absorption coefficient (>10^4/cm) means that even a thin layer is able to absorb most of the energy from incident sunlight. The layer of CdTe for the simulation is varied and can be considered to be depleted of charge carriers because of the relatively larger doping concentration of ITO-CdS. The CdTe thus acts as absorber layer in the solar cell.

Fig. 6 shows open-circuit voltage, short-circuit current and efficiency as a function of CdTe absorber thickness and doping level.

It is clear from Fig. 2a that to obtain an open circuit voltage close to or greater 1V the doping concentration should exceed 5×10^{15} atoms/cm^3. A large impurity concentration corresponds to an increased electric field strength which promotes charge separation. However, very high values of impurity concentration (greater than $1x10^{15}$/cm^3) can also enhance the recombination process limiting the short-circuit current, Fig. 2b. It is also evident that the possibility of bulk recombination increases for increased absorber layer thickness which saturates the short-circuit current. It should be noted that the overall conversion efficiency is strongly dependent on both the doping concentration and thickness of the CdTe layer. For thickness greater than 2 μm the efficiency is almost same and is independent of the doping concentration exceeding 1×10^{15}/cm^3. However, for CdTe thickness in the range of 0.5μm – 2μm there is a steep increase in efficiency. The smaller values of efficiency at low values of CdTe thickness can be attributed to two factors: lower absorption of photons and saturation of short-circuit current because of the reduced minority carrier diffusion length. Fig. 2c also suggests that for thickness beyond 2 μm the increment in efficiency is insignificant.

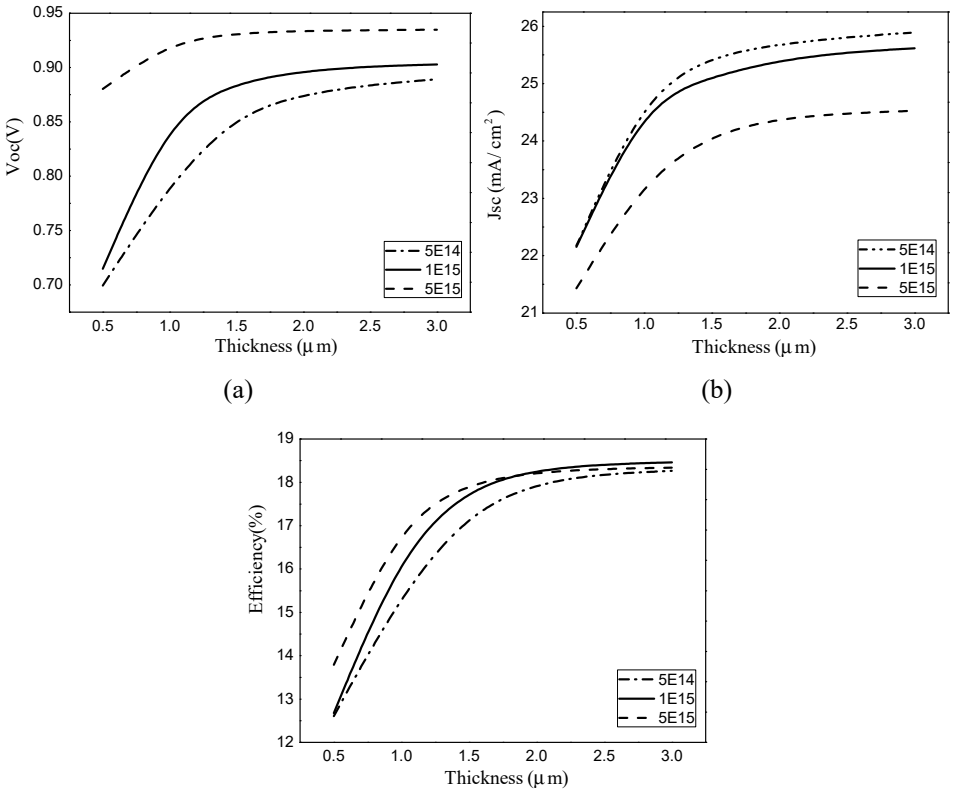

Fig. 2 – *Dependence of:* (a) *open-circuit voltage;* (b) *short-circuit current;* (c) *efficiency as a function of CdTe absorber thickness and doping level.*

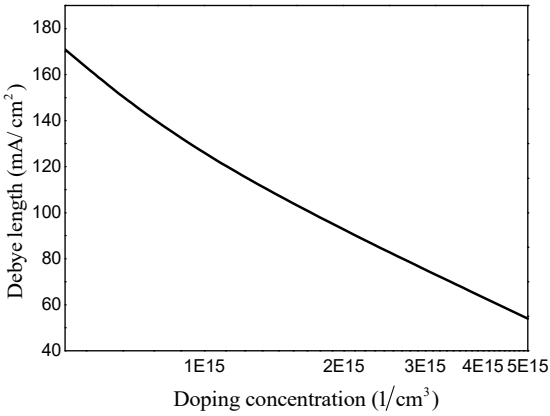

Fig. 3 – *Debye length as a function of CdTe absorber layer doping level.*

The Debye length (L_D) has been calculated [24] and is defined as the length over which the local electric field affects the flow of the charge carriers. The Debye length is inversely proportional to the square root of the doping concentration and therefore decreases as the carrier concentration increases (Fig. 3). According to the Schottky barrier model the charge carrier transit time through the depletion region is proportional to the square of the Debye length, clearly suggesting that for improved electron-hole separation the carrier transit time should be low.

3.2 Effect of defect density concentration

In the defect density model, there is an alteration in energy band structure at the depletion region because of the presence of trapped charge carriers in the defect states. Defect states play a major role in determining the overall performance of a solar cell. These states present in the bandgap of the material cause undesirable trapping of mobile charge carriers lowering the current density of the solar cell. In this paper, considering the worst case scenario, the defects were chosen to be located at the middle of the bandgap and the effect of defect density on the current and efficiency of the CdS/CdTe are reported.

The acceptor defect concentration of CdS window layer is varied from 1×10^{15} to 1×10^{19}/cm^3 while the donor defect concentration of the CdTe absorber layer is varied from 2×10^{11} to 2×10^{15}/cm^3. In both the cases it is found that the short-circuit current density increases when the defect density is reduced, Fig. 4a and 5a. For CdS window, when the defect density is decreased from 1×10^{19} to 1×10^{15}/cm^3 the efficiency of the cell increases from 17.25 to 20.04%, Fig. 4b. At the same time for the CdTe absorber, the decrease in defect density from 2×10^{15} to 2×10^{11}/cm^3 accounts for the increase in efficiency from 15.91 to 19.60%, Fig. 5b.

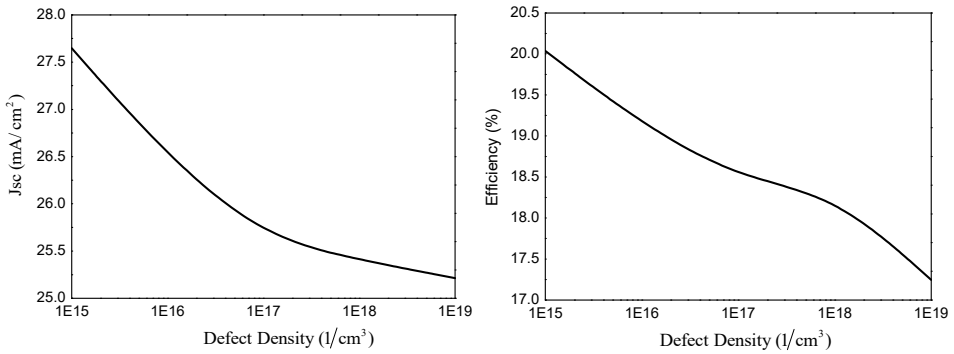

(a) (b)

Fig. 4 – *Effect of defect density concentration for the CdS window layer on the:* (a) *short-circuit current;* (b) *efficiency.*

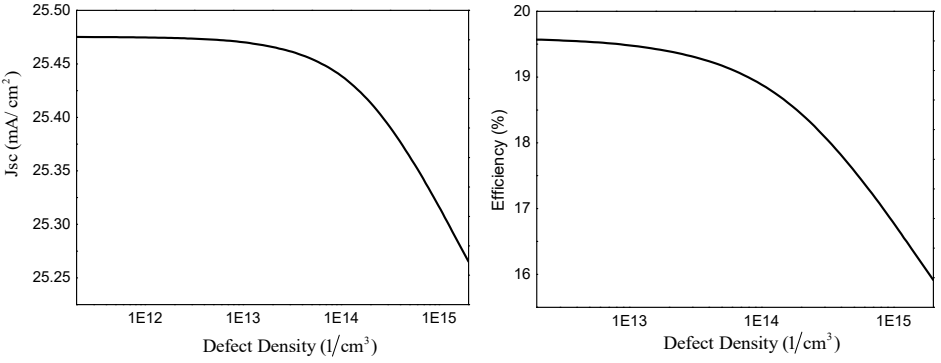

Fig. 5 – *Effect of defect density concentration for the CdTe absorber layer on the:* (a) *short-circuit current;* (b) *efficiency.*

3.3 Optimised solar cell

Based on the investigation the chosen values of doping concentration, thickness and defect states of CdS and CdTe layers are summarised in **Table 4.**

Table 4
Optimised material parameters of the different layers.

Layers	Thickness (μm)	Doping concentration ($1/cm^3$)	Defect State Concentration ($1/cm^3$)
CdS	0.05	Donor: 1×10^{19}	Acceptor: 1×10^{18}
CdTe	2.00	Acceptor: 1×10^{15}	Donor: 2×10^{14}

In order to achieve a greater value of V_{OC} high Quasi-Fermi Level splitting is a must, and can be obtained by choosing a low value of interface recombination and large value of carrier lifetime. Fig. 6 shows the energy band diagram of the proposed solar cell which represents the separation of Fermi Level into Quasi-Fermi levels of electrons and holes. The band bending at the CdS/CdTe interface suggests that space-charge region extends deep (1.1 μm) inside the CdTe region, which is in conformity with the difference of doping levels between these layers. There is a conduction band offset of $\Delta E_C = 0.2$ eV at the CdS/CdTe junction. The presence of the depletion region at the CdS/CdTe junction aids the movement of electrons in the conduction band and holes in the valence band enhancing the collection probability.

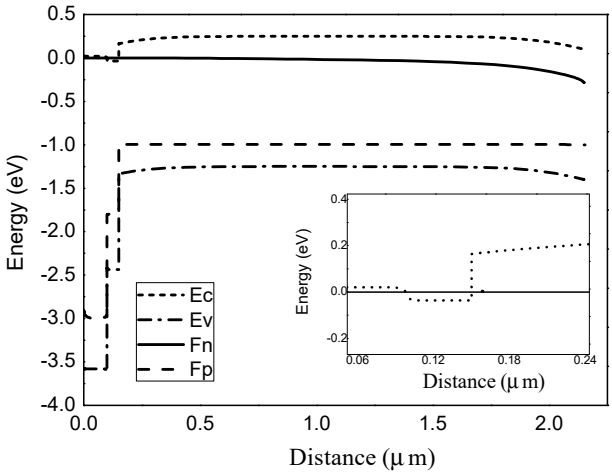

Fig. 6 – *Energy Band Diagram of the proposed CdS/CdTe cell under illumination; Inset: Conduction Band offset of* 0.2 eV *at the CdS/CdTe interface* (x = 0.15μm).

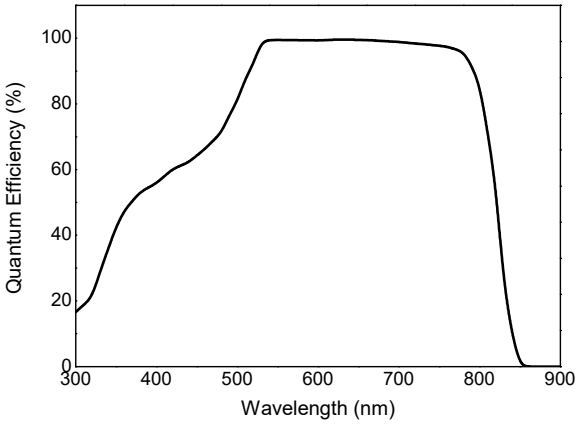

Fig. 7 – *Spectral response of the proposed CdS/CdTe cell.*

The spectral response (Fig. 7) is indicative of the fact that the cell's response diminishes for wavelengths below 525 nm which is in agreement with the poor blue response associated with CdS/CdTe based solar cells. Therefore, in general the thickness of CdS layer is always chosen below 100 nm. It should be emphasised here that the high frequency response of the proposed cell can be improved even further if the depth of CdS layer is reduced below 50 nm ignoring the practical constraints [18].

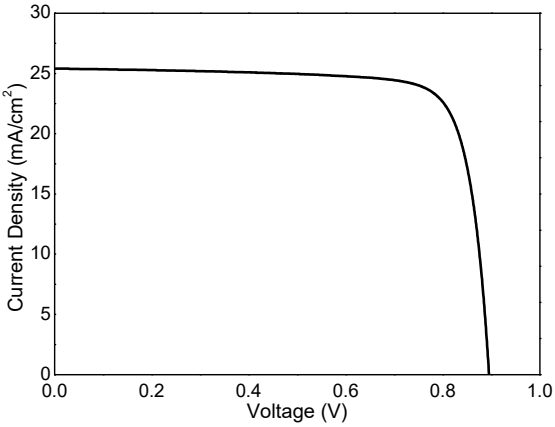

Fig. 8 – *Optimised current-voltage (I-V) characteristics of the CdS/CdTe photovoltaic cell.*

Fig. 8 shows the I-V characteristics of the proposed solar cell with the following extracted electrical characteristics: open-circuit voltage, V_{OC}, $V_{OC} = 0.8967\,\text{V}$, short-circuit current, J_{SC}, $J_{SC} = 25.406\,\text{mA}/\text{cm}^2$, fill factor, FF = 80.29% and efficiency is 18.29%.

3.4 Effect of working temperature on the I-V characteristics

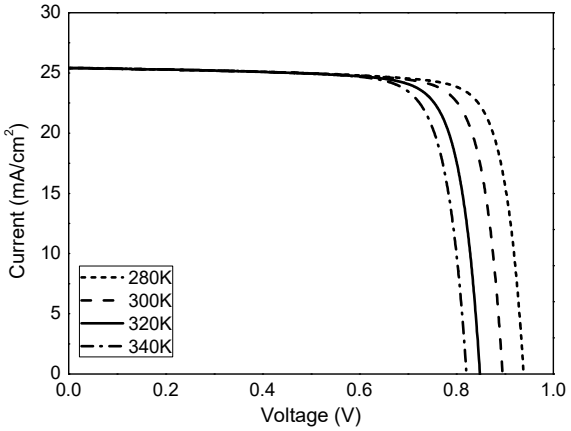

Fig. 9 – *Temperature effect on the I-V characteristics of the CdS/CdTe solar cell.*

Fig. 9 shows the dependence of the current-voltage characteristics on the working temperature of the solar cell. An increase in temperature reduces the bandgap of the semiconductor material following the relation [25]:

$$E_G(T) = E_G(0) - \frac{\alpha T^2}{T + \beta}, \tag{1}$$

where $E_G(T)$ is the bandgap at a particular temperature, $E_G(0)$ is the bandgap at 0 K, α and β are constants for a particular semiconductor.

In particular temperature increase has a prominent role in determining the decrease in open-circuit voltage of the solar cell, and is governed by the relation:

$$\frac{\mathrm{d}V_{OC}}{\mathrm{d}T} = \frac{V_{OC}}{T} + \frac{kT}{q}\left(\frac{\mathrm{d}J_{SC}}{J_{SC}\,\mathrm{d}T} - \frac{\mathrm{d}J_0}{J_0\,\mathrm{d}T}\right), \tag{2}$$

where J_{SC} is the short-circuit current density, k is the Boltzmann constant, q is the electronic charge and J_0 is the reverse saturation current density and is related to the diffusivity (D), diffusion length (L), doping concentration (N) as per the equation:

$$J_0 = \frac{qDn_i^2}{LN}. \tag{3}$$

In (3) the term n_i is the intrinsic carrier concentration which has a strong dependence on temperature and bandgap of the material, given by:

$$n_i^2 = BT^3 \exp\left(-\frac{E_G(0)}{kT}\right), \tag{4}$$

where B is a semiconductor material dependent constant.

3.5 Capacitance voltage (C-V) measurements

To verify the consistency of the results the capacitance-voltage measurements were made at four different frequencies. The total junction capacitance associated with the p-n junction is considered to be the sum of depletion and diffusion capacitance. At reverse bias voltages the depletion capacitance dominates the diffusion capacitance, whereas for forward bias the diffusion capacitance overrides the depletion capacitance. At zero bias voltage the capacitance of the cell is found to be 1.4 nF (Fig. 10). The expression for depletion capacitance is given as:

$$C(V) = A\sqrt{\frac{q\varepsilon\varepsilon_0 N}{2(V_{bi} - V)}}, \tag{5}$$

where A is the area of cross-section of the junction, q is the electronic charge, ε is the dielectric constant of the semiconductor, ε_0 is the permittivity of free space, N is the carrier density, V_{bi} is the built in electric field and V is the applied potential. From Fig. 10 it can be seen that the capacitance curve has $1/\sqrt{(V_{bi} - V)}$ dependence.

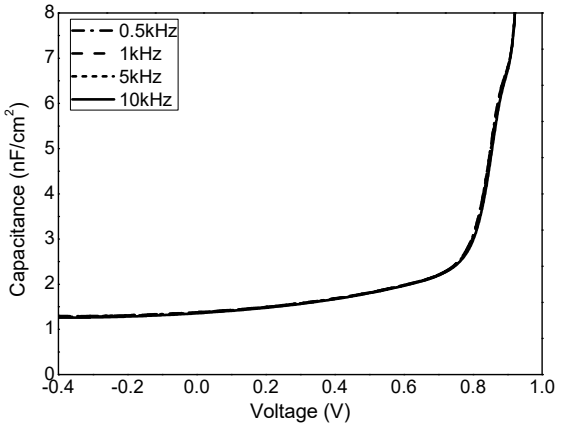

Fig. 10 – *Capacitance vs. Voltage plot of the CdS/CdTe photovoltaic cell.*

The data presented in Fig. 11 can be best interpreted using the Mott-Schottky equation (derived using equation (5)):

$$\frac{1}{C^2} = \frac{2}{q\varepsilon\varepsilon_0 A^2 N}(V_{bi} - V)\,. \tag{6}$$

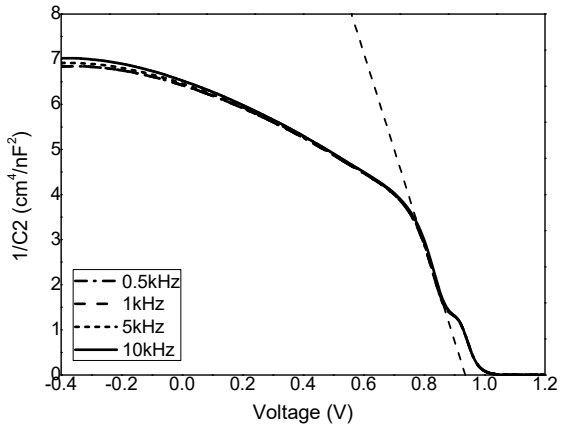

Fig. 11 – *Mott-Schottky plot of the CdS/CdTe photovoltaic cell.*

This equation generates a linear region which has a slope equivalent to the doping concentration. The intersection of the $1/C^2$ plot with the voltage axis yields the flat-band voltage of the cell. The carrier concentration can also be calculated by differentiating (6) and applying the formula:

$$N = \frac{2}{q\varepsilon\varepsilon_0 A^2} \frac{1}{\frac{\mathrm{d}(1/C^2)}{\mathrm{d}V}}. \tag{7}$$

The Mott-Schottky fit has a slope of –20 cm^4V^{-1}/nF^2 and intersects the x-axis at 0.93 V, which is the flat-band voltage of the CdS/CdTe junction. The negative slope of the plot suggests that the majority charge carriers are holes and the space charge region mostly occupies the p-type CdTe layer. Putting the appropriate values in equation (7), the carrier concentration is found to be $6.845\times10^{18}/cm^3$. The excess carrier density in CdTe layer is due to the photo-generated charge carriers upon exposure to sunlight of intensity 1000 W/m^2.

4 Conclusion

As part of the I-V measurements extensive numerical analysis has been done to understand the role of thickness and doping concentration of the CdS window and the CdTe absorber layer on the output. Taking into consideration the practical constraint associated with the minimum CdS thickness of 50 nm, it was found that the doping level of CdS had no significant impact on the PCE of the cell. It was also shown that for CdTe thickness the optimum doping concentration was $1\times10^{15}/cm^3$, and the efficiency had no enhancement beyond a thickness of 2 μm. The Debye length for the chosen CdTe doping concentration is 120.85 nm which is a reasonably low value meaning better charge separation and reduced recombination. It is also evident from the analysis that defect density in general always has a detrimental effect on both the short circuit current and PCE of the cell. The spectral response for shorter wavelengths has to be improved in order to achieve better efficiency yield. The optimised solar cell structure after accounting for various factors had an efficiency yield of 18.29%. The efficiency can be enhanced further by the introduction of a thin and highly doped electron back reflector layer to suppress the possible recombination loss at the back contact.

C-V profiling is an integral part of characterising semiconductor devices like solar cells and can be used to improve the device performance. Results from C-V characterisation yield information on threshold voltage, deletion layer width, and charge concentration. Yet, to the best of our knowledge, no theoretical report concerning the C-V numerical simulation of CdS/CdTe has been found in literature. To validate the repeatability of the results measurements were made at 0.5, 1, 5 and 10 kHz. The M-S plot showed that the threshold voltage of the device is 0.93 V and the cell had an excess carrier concentration of $6.844\times10^{18}/cm^3$ upon illumination of intensity 1000 W/m^2.

5 References

[1] Y.- J. Lee, J.L. Gray: Numerical Modeling of Polycrystalline CdTe and CIS Solar Cells, Proceedings of the 23rd IEEE Conference on Photovoltaic Specialists, Louisville, KY, USA, May 1993, pp. 586 – 591.

[2] X. Wu: High-Efficiency Polycrystalline CdTe Thin-Film Solar Cells, Solar Energy, Vol. 77, No. 6, December 2004, pp. 803 – 814.

[3] Y. Zhao, M. Boccard, S. Liu, J. Becker, X.- H. Zhao, C.M. Campbell, E. Suarez, M.B. Lassise, Z. Holman, Y.- H. Zhang: Monocrystalline CdTe Solar Cells with Open-Circuit Voltage Over 1 V and Efficiency of 17%, Nature Energy, Vol. 1, June 2016, pp. 1 – 7.

[4] A. Luque, S. Hegedus: Handbook of Photovoltaic Science and Engineering, 1st Edition, JohnWiley & Sons, Chichester, 2003.

[5] G.C. Morris, S.K. Das: Some Fabrication Procedures for Electrodeposited CdTe Solar Cells, International Journal of Solar Energy, Vol. 12, No. 1-4, 1992, pp. 95 – 108.

[6] V.M. Nikale, S.S. Shinde, C.H. Bhosale, K.Y. Rajpure: Physical Properties of Spray Deposited CdTe Thin Films: PEC Performance, Journal of Semiconductors, Vol. 32, No. 3, March 2011, pp. 033001 – 033007.

[7] T. Okamoto, Y. Matsuzaki, N. Amin, A. Yamada, M. Konagai: Characterization of Highly Efficient CdTe Thin Film Solar Cells by Low-Temperature Photoluminescence, Japanese Journal of Applied Physics, Vol. 37, No. 7, July 1998, pp. 3894 – 3899.

[8] N. Amin, K. Sopian, M. Konagai: Numerical Modelling of CdS/CdTe and CdS/CdTe/ZnTe Solar Cells as a Function of CdTe Thickness, Solar Energy Materials and Solar Cells, Vol. 91, No. 13, August 2007, pp. 1202 – 1208.

[9] D.L. Batzner, A. Romeo, H. Zogg, R. Wendt, A.N. Tiwari: Development of Efficient and Stable Back Contacts on CdTe/CdS Solar Cells, Thin Solid Films, Vol. 387, No. 1-2, May 2001, pp. 151 – 154.

[10] I.M. Dharmadasa: Latest Developments in CdTe, $CuInGaSe_2$ and GaAs/AlGaAs Thin Film PV Solar Cells, Current Applied Physics, Vol. 9, No. 2, March 2009, pp. e2 – e6.

[11] J. Sites, J. Pan: Strategies to Increase CdTe Solar-Cell Voltage, Thin Solid Films, Vol. 515, No. 15, May 2007, pp. 6099 – 6102.

[12] J. Han, C. Fan, C. Spanheimer, G. Fu, K. Zhao, A. Klein, W. Jaegermann: Electrical Properties of the CdTe Back Contact: A New Chemically Etching Process based on Nitric Acid/Acetic Acid Mixtures, Applied Surface Science, Vol. 256, No. 20, August 2010, pp. 5803 – 5806.

[13] N. Romeo, A. Bosio, R. Tedeschi, A. Romeo, V. Canevari: A Highly Efficient and Stable CdTe/CdS Thin Film Solar Cell, Solar Energy Materials and Solar Cells, Vol. 58, No. 2, June 1999, pp. 209 – 218.

[14] M.A. Matin, M.M. Aliyu, A.H. Quadery, N. Amin: Prospects of Novel Front and Back Contacts for High Efficiency Cadmium Telluride Thin Film Solar Cells from Numerical Analysis, Solar Energy Materials and Solar Cells, Vol. 94, No. 9, September 2010, pp. 1496 – 1500.

[15] J. Britt, C. Ferekides: Thin-Film CdS/CdTe Solar Cell with 15.8% Efficiency, Applied Physics Letters, Vol. 62, No. 22, May 1993, pp. 2851 – 2852.

[16] N. Romeo, A. Bosio, R. Tedeschi, V. Canevari: Back Contacts to CSS CdS/CdTe Solar Cells and Stability of Performances, Thin Solid Films, Vol. 361, February 2000, pp. 327 – 329.

[17] N. Romeo, A. Bosio, A. Romeo: An Innovative Process Suitable to Produce High-Efficiency CdTe/CdS Thin-Film Modules, Solar Energy Materials & Solar Cells, Vol. 94, No. 1, January 2010, pp. 2 – 7.

[18] N. Amin, M.A. Matin, M.M. Aliyu, M.A. Alghoul, M.R. Karim, K. Sopian: Prospects of Back Surface Field Effect in Ultra-Thin High-Efficiency CdS/CdTe Solar Cells from Numerical Modeling, International Journal of Photoenergy, Vol. 2010, February 2011, pp. 578580- 1– 578580- 8.

[19] H. Fardi, F. Buny: Characterization and Modeling of CdS/CdTe Heterojunction Thin-Film Solar Cell for High Efficiency Performance, International Journal of Photoenergy, Vol. 2013, July 2013, pp. 576952-1 – 576952-6.

[20] S. Khosroabadi, S.H. Keshmiri, S. Marjani: Design of a High Efficiency CdS/CdTe Solar Cell with Optimized Step Doping, Film Thickness, and Carrier Lifetime of the Absorption Layer, Journal of the European Optical Society- Rapid Publications, Vol. 9, December 2014, pp. 14052-1 – 14052-6.

[21] R. Safa Sultana, A.N. Bahar, Md. Asaduzzaman, Kawsar Ahmed, C. Cameselle: Numerical Modeling of a CdS/CdTe Photovoltaic Cell based on ZnTe BSF Layer with Optimum Thickness of Absorber Layer, Cogent Engineering, Vol. 4, No. 1, April 2017, pp. 1318459 – 2 – 1318459-11.

[22] M. Burgelman, P. Nollet, S. Degrave: Modelling Ploycrystalline Semiconductor Solar Cells, Thin Solid Films, Vol. 361, February 2000, pp. 527 – 532.

[23] Z. Fang, X.C. Wang, H.C. Wu, C.Z. Zhao: Achievements and Challenges of CdS/CdTe Solar Cells, International Journal of Photoenergy, Vol. 2011, October 2011, pp. 297350-1 – 297350-8.

[24] L. Kosyachenko: Efficiency of Thin-Film CdS/CdTe Solar Cells, Solar Energy, Edited by R. Rugescu, IntechOpen, 2010.

[25] D. Pal, R. Adhikary: Studies on the Performance of a GaInP/GaAs Tandem Solar Cell at Elevated Temperatures, International Journal of Engineering and Manufacturing, Vol. 9, No. 1, January 2019, pp. 38 – 46.